Chapter 1 Overview

1. 1 Total System

The purpose of the project is to promote all the related scientific and engineering fields, by making the full use of the secondary beams, including the neutrons, the muons, the Kaons, the neutrinos, and so forth, which can be efficiently produced by the proton beams. In order to produce the intense secondary beams, the beam power should be as high as possible, while the beam energy should sufficiently exceed the thresholds for the efficient production of the secondary beams. The time structure of the proton beams is another important factor in order to conduct the fruitful experiment [1]. The major requirements for the accelerator can be summarized as follows.

1) The accelerator complex should provide the 1-MW beam with a repetition rate of 25 Hz and a pulse length less than 1 μs to the full use of pulsed spallation neutrons. For producing the spallation neutrons efficiently the beam energy should be higher than several hundred MeV and lower than several GeV.
2) It should provide the several ten GeV beams with a beam power of 0.75 MW for nuclear and particle physics experiments, being extracted both slowly and fast.

The energies and the currents of the beam-power front proton machines are shown in Fig. 1.1. It is interesting to see that the present beam power front is approximately 0.1 ~ 0.2 MW for both ~ 1 GeV and several ten GeV machines. Perhaps, this is not accidental as detailed later in Sec. 1.2. There seems to be technical reasons for this. Then, we have to solve the problems which at present limit the beam power.

In order to meet the requirement 2) the cascade system is most suitable. A large-scale of the cascade system for this purpose was first realized by the present KEK-PS, comprising the 40-MeV linac, the 500-MeV booster synchrotron, and the 12-GeV proton synchrotron. Needless to say, the beam power of the KEK-PS is too weak for the present purpose. For the power up, one has to increase the beam energies for both the extraction and the injection. The former is for the beam power itself, while the latter is for increasing the beam current by easing the space charge effect at injection. The extraction energy of the MR is chosen 50 GeV, while the injection energy is 3 GeV. The extraction energy is perhaps optimized by taking into account various factors including the full use of the site area, the cost performance for the scientific outputs, the ratio of the extraction energy to the injection one, and so forth. The injection energy, that is, the extraction energy of the booster RCS, is

ideal for the production of the spallation neutrons, the efficiency of which starts to be decreased at this proton energy. This factor is taken into account to choose the RCS energy. It is interesting to note that the present project with the parameters thus determined looks a kind of scale up of the KEK-PS.

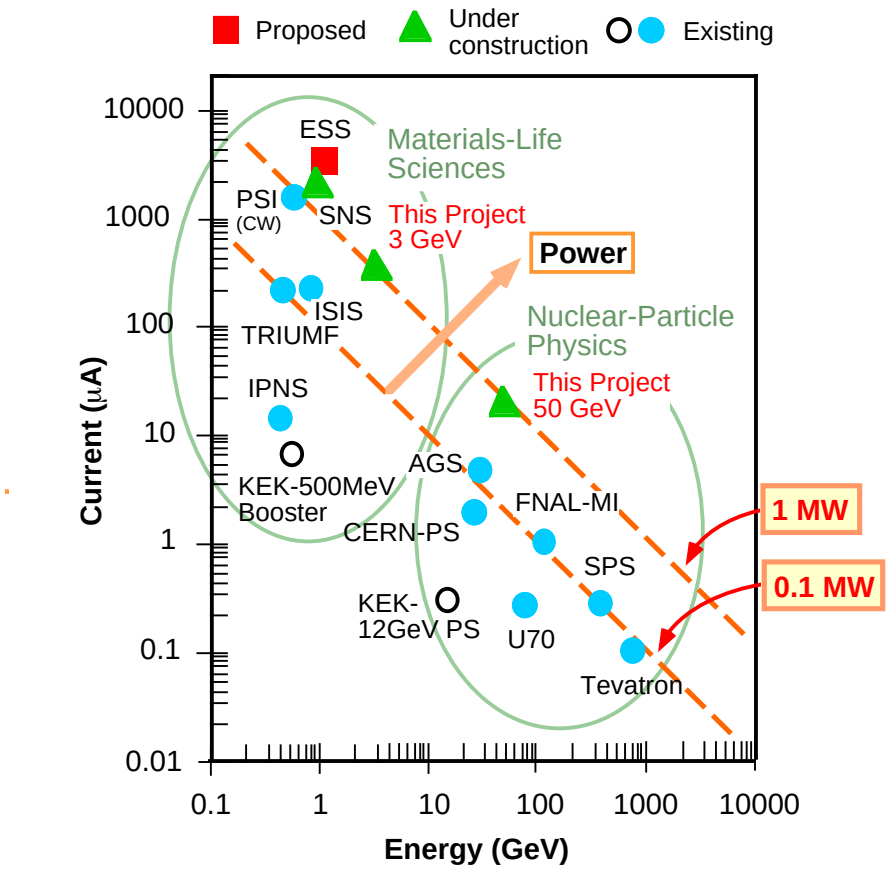

FIG 1.1: Beam energy, beam current, and beam power of world's proton machines

In contrast to the Spallation Neutron Source (SNS) project in US or the European Spallation Neutron Source (ESS), which comprises the full-energy linac and the compressor accumulator ring (AR), the present project is to produce the high-power pulsed beams by means of the RCS. After the beams are injected from a linac to a ring, the beams will be rapidly accelerated in the ring. The requirement 1) is thus fulfilled. This scheme may be more powerful than the others. The advantages and disadvantages of the RCS scheme versus the AR scheme are discussed in Sec. 1. 2.

More specifically, the main beam parameters are summarized [2-4] in the following table.

Table 1.1. Main Beam Parameters

Linac	
Ions	Negative Hydrogen
Energy for RCS injection	400 MeV
Energy for ADS	600 MeV
Peak Current	50 mA
Beam Pulse Length	500 μs
Repetition Rate	50 Hz
RCS	
Extraction Beam Energy	3 GeV
Repetition	25 Hz
Average Beam Current	333 μA
Extraction Scheme	Fast
MR	
Extraction Beam Energy	50 GeV
Average Beam Current	15 μA
Repetition	0.3 Hz
Extraction Scheme	Fast, and Slow

The H^- beams produced in the negative ion source are accelerated to 400 MeV. The beams are chopped with a chopping rate of 56 %. The two buckets in the RCS are waiting for the beam injection. The injection continues for 500 μs, while the magnet system of the RCS is sinusoidally oscillating with a frequency of 25 Hz. After the beams are accelerated to 3 GeV, the beams are fast extracted for most of times to the muon production target and neutron production target located in a series in the Materials and Life Science Experimental Hall. Every three seconds, however, the beams are extracted to the MR. The two buckets among the nine buckets in the MR accept the two bunches from the RCS at a time. This is repeated four times as shown in Fig. 1.2. After the last two bunches are injected, the ramping is immediately started as shown in Fig. 1.3. After the beams are accelerated to the 50 GeV, the beams are slowly extracted for 0.7 s to the Nuclear and Particle Physics Experimental Area in one case. In the other case, the beams are fast extracted to the neutrino

production target. After the beams are extracted, the magnetic fields are decreased down to the values for the injection.

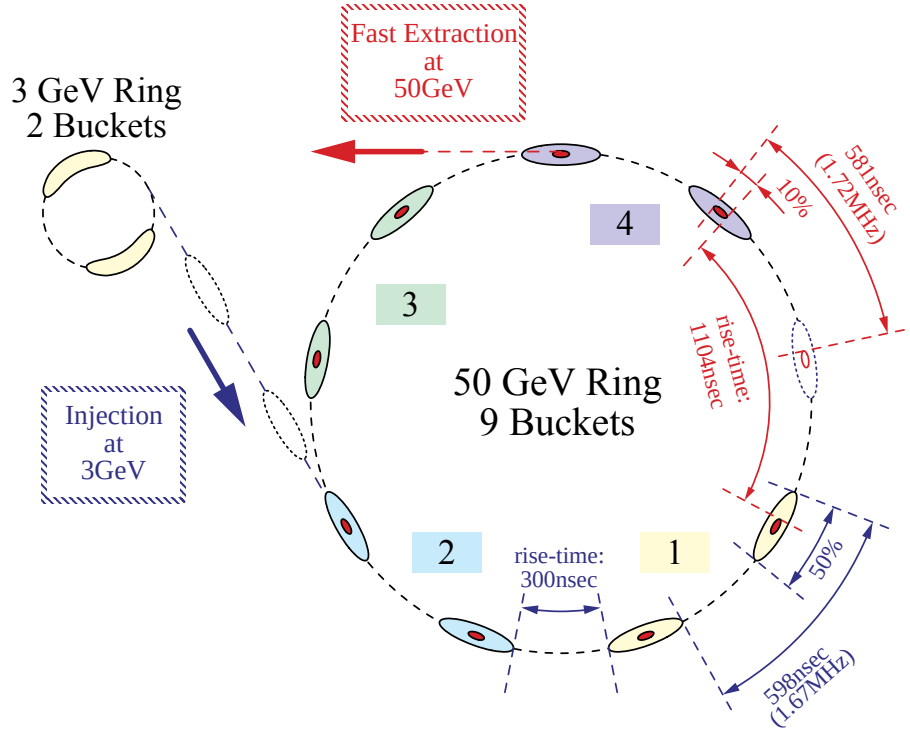

FIG 1.2: Injection scheme from the RCS to the MR

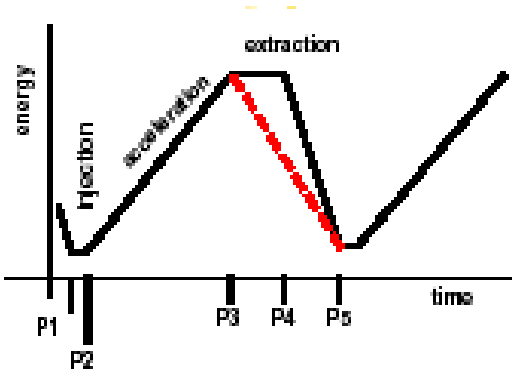

P1 - P2(injection)	0.14 s
P2 - P3(acceleration)	1.9 s
P3 - P4(extraction)	0.7 s
P4 - P5	0.9 s
total	3.64 s
slow extraction of 30GeV	
duty factor	0.20
average current	15μA

Fig. 1.3. Acceleration cycle of the MR

In addition to the spallation neutron source and the nuclear and particle physics experimental areas, the accelerators provide the beams to the experimental areas for the muon science and the accelerator-driven nuclear waste transmutation system (ADS). The muon production target is located in a series in front of the neutron production target within the Materials and Life Science Experimental Area as mentioned above. Thus, the requirement for the accelerator complex from the muon science is only the beam pulse length (100 ns) in this case. Fortunately, this requirement is consistent with the present accelerator scheme. Ideally speaking, the shorter bunch length is sometimes requested for the muon experiment. This request, however, is not consistent with that from the neutron experiment. Although the shorter bunch can be realized by the manipulation of the RF voltages, the beam power of 1 MW is very difficult to achieve with the shorter bunch length.

For the ADS, the continuous wave (CW) beams are ultimately required. The linac to be operated in both the pulsed mode and the CW mode has been once proposed for the NSP, since the CW proton linac can be operated in the pulsed mode. However, this kind of linac is very expensive. If the peak beam current in the CW mode is lower, by a factor of three or more, than that in the pulsed mode, the linac may be more expensive than two linacs, that is, CW one and pulsed one. For this reason, the ADS experiments, which are costly compatible with the pulsed neutron source, are limited to those which use the pulsed beams. Since the ADS experiments at least requested the spallation neutrons, the beam energy exceeding 600 MeV is required. Since the pulse length of the 3-GeV beam from the RCS is too short for the ADS experiment, the 600-MeV linac is necessary for the ADS experiment. The choice of the linac scheme is discussed in Sec. 1. 3.

1. 2 Advantages and Disadvantages of the RCS versus AR

Since the pulsed spallation neutron source is one of the main facilities in the present accelerator complex, the choice of the accelerator scheme for the neutron source is a very important issue. The advantages of the RCS scheme over the AR scheme are simply summarized by the lower beam current and lower injection energy for the same beam power [1]. Specifically, the beam current of the 3-GeV RCS is only one third as high as that of the 1-GeV AR. Needless to say, the low-energy linac is less expensive and smaller than the high-energy linac.

Furthermore, if the injection energy is 400 MeV like the present case, the ratio of the allowed beam loss to the beam current during the injection to the RCS is 7.5 times as

high as that to the AR, if the same beam loss power is assumed. Since the injection process is the indispensable main source for the beam loss among the various processes including the acceleration and extraction, this advantage is very important. In many cases the beam current is limited by the allowed beam loss power (uncontrollable), which gives rise to the radioactivity of the accelerator components. The hands-on maintenance of the accelerator components are usually assumed for the design of the accelerators. This limits the allowed radioactivity, which is usually proportional to the beam loss power. If the injection beam energy is lower than 500~600 MeV, the beam loss power is more allowed than the case of the higher energy, since the radioactivity produced by the beam is lower than estimated by assuming its proportionality to the beam power.

Here, one may also imagine the possible reason why the present beam power front is common over the wide range of the beam power. Suppose that the obtainable ratio of the beam loss to the beam current is limited by the present accelerator technology. Then, the limited beam power becomes the same for all the machines, since the radioactivity is approximately proportional to the beam loss power. This implies that we have to develop or to use new technologies for decreasing the ration of the beam loss to the beam current by an order of magnitude, if one wishes to increase the beam power by an order of magnitude. Some developments will be described in the following subsections.

As detailed in Sec. 2.2.8, the RCS scheme is more immune against the ep instability. Actually, no ep instability was observed in ISIS (the 70-MeV linac with the 800-MeV RCS), while the instability is one of the most serious problems in LANSCE (the 800-MeV linac with AR).

The disadvantages of the RCS scheme compared with the AR scheme are summarized as follows.

1) The lower injection energy in turn implies the higher space charge effect. The large aperture magnets are required in order to overcome the space charge effect. Big magnets and powerful power supplies are necessary. The large apertures give rise to large fringing fields.
2) The powerful RF accelerating system is necessary.
3) The ceramics vacuum chamber should be used to avoid the eddy current effect. Then, the RF shields should be attached to the ceramics vacuum chambers in order to prevent the electromagnetic waves from radiating from the beams.
4) Stranded coils should be used to overcome the eddy current effect on the magnet coils in some cases.

5) Precise magnet field tacking is necessary for each family of magnets.

One must solve all these problems. However, nothing is a fatal problem, although the system will become very complicated.

If one considers the above advantages and disadvantages of the two schemes, it is still controversial which scheme is more promising for producing the MW beam power. The further powerful sources may be realized by combining the RCS with the high-energy linac in future. In this case, the powerful RCS should be developed for the future accelerator technology.

1. 3 Features of the Linac Design

The linac comprises a volume-production type of H^- ion source, a 50-keV low-energy beam transport (LEBT), a 3-MeV, 324-MHz Radio-Frequency Quadrupole (RFQ) linac, a 50-MeV, 324-MHz Drift-Tube Linac (DTL), a 200-MeV, 324-MHz Separated DTL (SDTL), and a 400-MeV, 972-MHz high-energy linac [5-7] as shown in Fig. 1.4. Table 1.2 summarizes the main parameters. The linac will be operated at a repetition rate of 50Hz. The 400-MeV beam is transported and injected to the RCS at a repetition rate of 25 Hz. At the other half of the repetition, the 400-MeV beam is further accelerated to 600MeV and is used for the ADS.

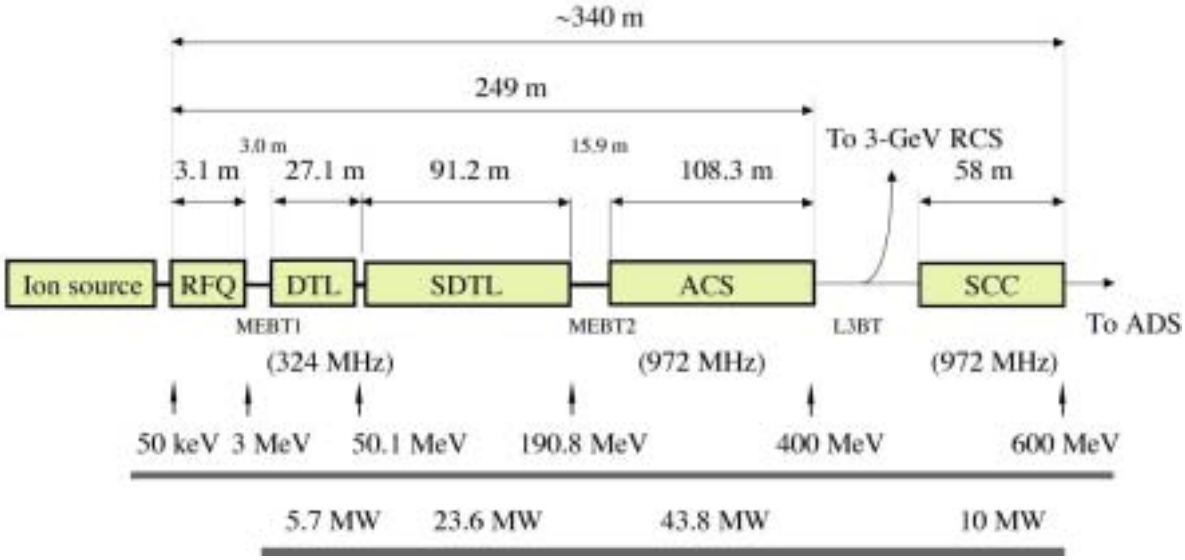

FIG. 1.4: Accelerating scheme of the linac

Table 1.2 Main parameters of the 600-MeV linac.

Energy	600 MeV	
Repetition	50 Hz	
Beam Pulse Length	500 μs	
Chopping Rate	56 %	
RFQ, DTL, SDTL Frequency	324 MHz	
ACS, SCC Frequency	972 MHz	
Peak Current	50 mA	
Linac Average Current	1.25 mA	
Average Current after chopping	700 μA	
Total Length	249 m	(up to 400 MeV)
	340 m	(up to 600 MeV)

H^- Ion Source

Type	Volume-Production Type
Peak Current	55 mA
Normalized Emittance (90%)	0.67 π mm mrad
Extraction Energy	50 kV

RFQ

Energy	3 MeV
Frequency	324 MHz

DTL

Energy	50 MeV
Frequency	324 MHz
Focusing Quadrupole Magnet	Electromagnet
Total Length	27 m
The Number of Tanks	3

SDTL

Energy	191 MeV
Frequency	324 MHz
Total Length	91 m
The Number of Tanks	32
The Number of Klystrons	16

ACS

Energy	400 MeV
Frequency	972 MHz
Total Length	108 m
The number of Tanks	46
The Number of Klystrons	23

SCC

Energy	600 MeV
Frequency	972 MHz
The number of cells in one tank	9

Tne number of tanks per cryomodule	2
The total number of cryomodules	11
Total Length of cryomodules	58 m

We have the following conflicting requirements for the linac design. The higher accelerating frequency is preferable, since the lower bunch current and the short focusing period arising from the higher frequency are both advantageous regarding the space charge effect. The higher frequency is also advantageous regarding the discharge limit of the electric field gradient, the shunt impedance, and the size of the RF components including the klystrons. All imply the better cost performance. On the other hand, the electromagnet system is preferable in order to keep the flexible knob. Both the equipartitioning and constant phase advance are realized in this case. The possibly dangerous parametric resonance can also be avoided. However, the large size of the drift tube is necessary in order to contain the electro quadrupole magnets. Then, the frequency must be decreased for the large drift tube.

We have developed the smallest-possible electro quadrupole magnets. The electromagnet coils are produced by fully using the electroforming method and the wire cutting. In this way, it becomes possible to use a frequency of 324 MHz for the DTL starting from 3 MeV. Definitely, the klystrons can be used for this frequency. However, the huge power feeding system is necessary for exciting these electromagnets.

Another problem arising from the high accelerating frequency is that the accelerating energy of the RFQ linac is quite limited (2 ~ 2.5 MeV for ~400MHz), since the four-vane type of the RFQ cannot exceed four times as long as the free-space wave length. This problem is solved by the invention of the π-mode stabilizing loop (PISL), which is also used for the SNS. The PISL's eliminate any effect of the deflecting field, resulting in the high quality of the accelerating and focusing fields.

Another feature of the linac design is that the longitudinal transition (200 MeV from SDTL to ACS) is separated from the transverse transition (50 MeV from DTL to SDTL). It is well known that the beam loss and beam quality degradation arise at the transitions. The separation of the two transitions give us more flexibility in order to avoid the mismatching at the transition, which gives rise to the halo formation.

It should be emphasized that the linac is used as an injector to the RCS. The most stringent requirement for this purpose is the accuracy of the beam momentum ($\Delta p/p = \pm 0.1\%$ (100%)). Both the 1% amplitude control and the 1˚ phase control should be realized

for this requirement. Also, the 99 % emittance (normalized) should be 3~5 π mm mrad. Then, the alignment of 0.05 ~ 0.1 mm is necessary for the quadrupole magnets.

In this context, the axial symmetry is perhaps important. This is one of the reasons for developing the Annular-Ring Coupled Structure (ACS) [8] for the high-energy linac structure. The axial symmetry also implies the easy manufacturing and the mechanical stability of the structure.

The medium-energy beam transport (MEBT) is another important component in the proton linac, in particular for the injector linac. First of all, the beam from the RFQ should be matched to the DTL both longitudinally and transversely. Second, this is the place where one can chop the beam, for the phase of which the ring RF separatrix cannot accept. The chopping is very difficult to do, since the chopping field should rise and fall, respectively, in between the two bunches. Otherwise, the beams partly deflected by the chopper would be accelerated, eventually giving rise to the high-energy beam loss. The RF chopper has been devised, and developed for this. Another difficulty in the chopper is that any scraper or stopper cannot stand the beam loss of all the chopped beams. The beams will be partly chopped before entering the RFQ linac, by decelerating the beam below the energy acceptance of the RFQ.

We are developing the ion sources both with and without cesium. At first we attempted the ion source without cesium, that is, purely volume production, since we prefer cesium-free ion source in order to avoid the possible decrease in the discharge limit of the following RFQ. However, the peak beam current of the cesium-free ion source is limited to 33 mA so far. Further improvement of the cesium-free ion source is under way. On the other hand, the cesium-seeded ion source being developed as a back up (of course, useless, if the RFQ cannot allow the use of the cesium) has already produced sufficient peak beam current. After the arc discharge power supply is upgraded, the peak beam current was increased in proportion to the arc power up to 70 mA (above the required value) with an aperture size of 8 mmϕ. The emittance measured is small enough. At present the effort is concentrated on the increase in its lifetime, which is one half of the required value.

Finally, we will discuss about the choice between the superconducting (SC) linac and the normal-conducting (NC) linac (sometimes, referred to as the room-temperature linac). The obtainable field gradient in the SCC has been recently improved, mainly owing to the state-of-art surface electropolishing technique [9]. Then, one can decrease the linac length for the same energy by using the SC linac. In addition, the higher field gradient

implies the larger longitudinal acceptance or the stronger longitudinal focusing, being more immune against the effect of the space charge. For these reasons we have again seriously evaluated the feasibility of the use of the SCL from 200 MeV to 400 MeV.

The required phase and amplitude accuracy of each cell and each tank (0.1˚ and 0.1 % to 1˚ and 1 %, respectively, being dependent upon the kind of the errors) is much severer for the RCS injection than required just for the ADS. The deviation in Δp/p should be around 0.1 percent. Therefore, the Lorentz detuning which becomes dynamic under the pulse operation should be accurately compensated. The SCC has been recently power-tested with the same pulse mode as required. The detuning is periodic from pulse to pulse. The amount of the static detuning was in agreement with the simulation within a few percent [10].

This detuning will be accurately compensated, if one uses a system of one SC cavity per one klystron. However, a system of two SC cavities per one klystron is only competitive in cost with the normal conducting (NC) system, if one uses the SCL for the acceleration from 200 MeV to 400 MeV. Therefore, the feasibility of the 400-MeV SCL as an RCS injector is dependent upon how similar the detunings of the two cavities are to each other.

It is recently realized that the high field gradient imposes further severe phase-amplitude control for the same deviation of the beam energy. For the same reason as the larger acceptance, the random kick or walk and the synchrotron oscillation during the course of the acceleration through the higher field gradient cavities becomes larger in the direction of the Δp/p in the longitudinal phase space. Under the presence of the Lorentz detuning the field control of the SCL is obviously much harder than the NC linac. For this reason, we have finally decided to use the NC linac up to 400 MeV.

The commissioning of the 3-MeV RFQ linac and MEBT has been started March, 2001. The beam transmission through the RFQ was in agreement with the designed value.

1. 4 Features of the RCS Design

We have chosen the lattice with three-folding symmetry. We need three long straight sections. One is dedicated to the long RF acceleration section, another to the injection and collimation, and the other to the extraction. The latter two sections will suffer from a lot of radioactivity, in particular, the injection/collimation section. It is preferable to

keep the RF section apart from these radioactive sections, since the maintenance of the RF components are usually required more frequently than other components.

The circumference of the RCS is limited by two factors. One is the beam pulse length of less than 1 μs for the neutron production, and the other is the circumference of the MR. As seen from Fig. 1.5, the present circumference for the MR is perhaps the maximum, if one attempts to keep the MR within the campus. If one increases the circumference of the RCS, the number of the beam transfer from the RCS to the MR must be decreased, resulting in the decrease in the beam current of the MR.

Once the circumference of the RCS is thus limited, the three-folding symmetry should be taken in order to keep one long straight section for the sufficient RF acceleration. Although the advantages and the disadvantages of the three-folding symmetry have been investigated in comparison with the four-folding symmetry, we finally decided to use the three-folding symmetry partly for this reason. Another reason is that the lattice with the three-folding symmetry is geometrically matched to the landform rather than the four-folding symmetry.

Other features incorporated in the lattice design are as follows. First, the straight sections are made dispersionless in order to avoid the synchrobetatron coupling. Second, the transition energy is chosen far above the operation energy.

The disadvantages of the RCS have been discussed in Sec. 1.2 in comparison with the AR scheme. The RCS design should solve these problems. First of all, the space charge limit on the beam current should be increased as much as possible. For this purpose, we attempt to increase the beam emittance as large as possible, keeping the gap of the bending magnets fixed. Perhaps, this is most cost-effective method. Specifically, we set the gap of the bending magnets as 210 mm. Then, we attempted to make the beta function there as small as possible. As a result, we could keep the physical aperture of 486 π mm mrad. The collimator acceptance was chosen two third as wide as the physical aperture in order to restrict the beam loss at the collimator. Finally, the painting emittance of 216 π mm mrad was chosen two third as wide as the collimator acceptance. This implies that the emittance growth is allowed up to 1.5 times after the injection.

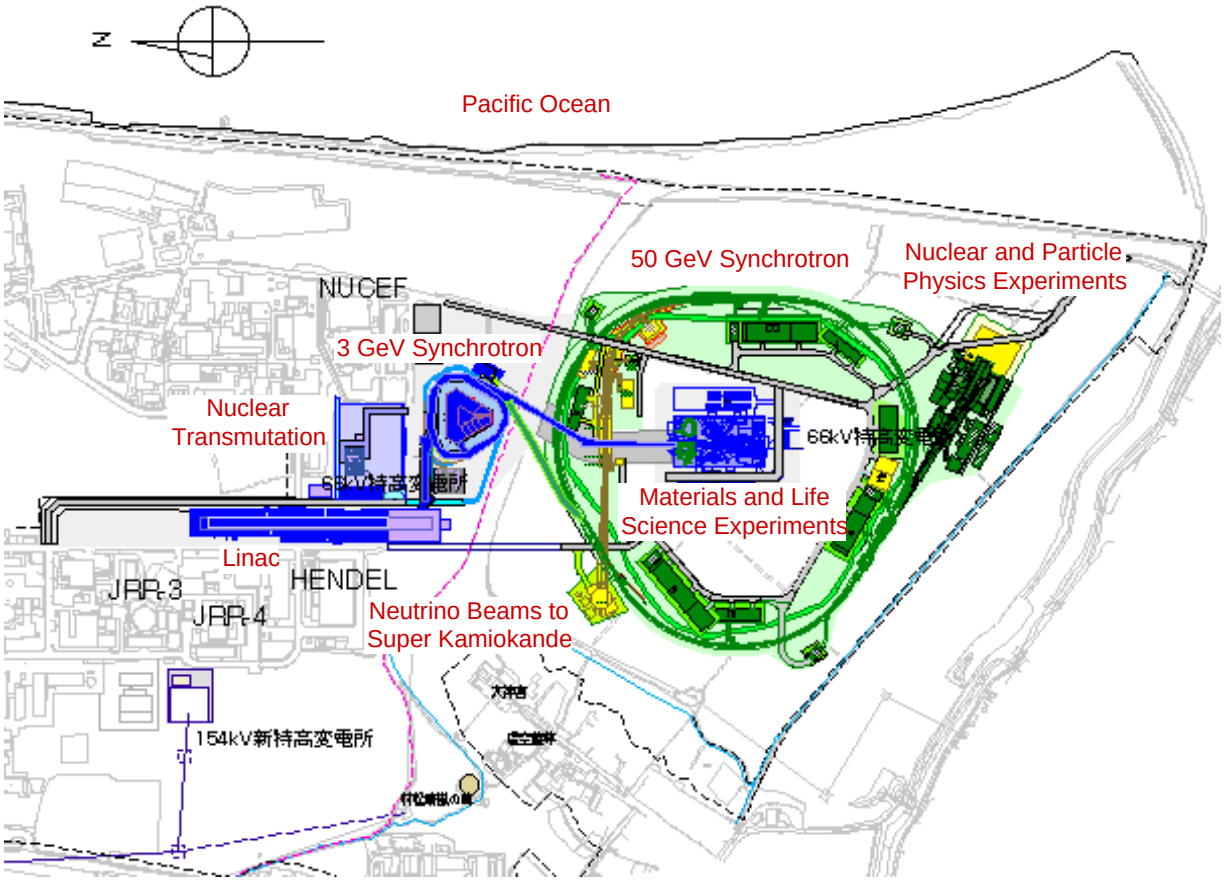

FIG 1.5: Plan view of the facility

Table 1.3 Main parameters of the 3-GeV synchrotron.

Energy	3 GeV
Beam Intensity	8.3 x 10^{13} ppp
Repetition	25 Hz
Average Beam Current	333 μA
Beam Power	1.0 MW
Circumference	348.333 m
Magnetic Rigidity	3.18 ~ 12.76 Tm
Lattice Cell Structure	(3-Cell FODO x 2module arc + 3-Cell Straight) x 3
Typical Tune	(6.68, 6.27)
Momentum Compaction Factor	0.012 (no transition below 3 GeV)
Transition γ	9.17
Total Number of Cells	27
The Number of Bending Magnets	24
Magnetic Field	0.27 ~ 1.1 T
The Number of Quadrupoles	60
Maximum Field Gradient	4.6 T/m

Harmonic Number		2
RF Frequency		1.36 ~ 1.86 MHz
Average Circulating Beam Current		9 ~ 12.4 A
RF Voltage		467 kV
RF Voltage per Cavity		42 kV (14 kV/gap)
The Number of RF Cavities		11 (+1)
Painting Emittance at Injection		216 π mm.mrad
Collimator Acceptance		324 π mm.mrad
Physical Aperture		486 π mm.mrad
Beam Emittance at Extraction		81 π mm.mrad
Bunching Factor with 2nd harmonic		0.41
Incoherent Tune Shift		0.16
Bunching Factor without 2nd harmonic		0.27
Incoherent Tune Shift		0.24
Bending	The Number of Magnets	24
	Gap Height	210 mm
	Good Field Region	240 mm
Quadrupole	The Number of Magnets	60
	The Number of Families	7
	Bore Diameter	290, 330 mm
	Bore Diameter at Inj/Ext	410 mm
Sextupole	The Number of Magnets	18
	The Number of Families	3
	Bore Diameter	290, 330 mm

The measure of the space charge effect is represented by the incoherent Laslett tune shift (spread). The value of the tune shift for the beam power of 1 MW is 0.24 with a bunching factor of 0.27, while it will come down to 0.16, if the bunching factor is improved to 0.41 by introducing the second harmonics into the RF accelerating field. Although the emittance growth should be carefully estimated on the basis of the beam simulation as detailed in Sec. 2.2.5, the tune shift of 0.16 looks reasonable for keeping the emittance growth within 1.5 times.

Taking all of these features into the lattice design, we have seven families of power supplies for quadrupole magnets. As mentioned in Sec. 1.2., the precise tracking of each of families is necessary. It is really a technical challenge how to precisely track this large number of families of the magnets.

One of the most difficult problems inherent to the high-energy RCS was solved by the innovative development of the accelerating cavity loaded with magnetic alloy(MA)[11], one of which is FINEMET. This cavity can generate the field gradient of over 50 kV/m (potentially over 100 kV/m) which is several times as high as conventional ferrite-loaded

cavities. For this reason the RF system becomes a reasonable size even for the high-energy RCS. Further power test and beam test of the MA-loaded cavities are being continued after several successful experiments.

As an injector the RCS has to match its beam longitudinally for the injection to the MR. For this reason the transition gamma should be much higher than 3 GeV, although the ring circumference becomes longer than the low transition gamma lattice. In addition the beam should be elongated in order to avoid a fast blow up just after the injection.

1. 5 Features of the MR Design

The striking feature of the MR lattice is the choice of the imaginary transition gamma. The imaginary transition gamma is realized by the missing bend method, in which the beta modulation is relatively small. The missing bend structure generates the negative dispersion at bending magnets, resulting in the imaginary transition gamma. Similarly to the RCS, we make the dispersionless straight section in order to avoid the synchro-betatron coupling.

The beam emittance at the injection is chosen as 54 π mm mrad, since it corresponds to a Laslett tune shift of – 0.14 with a bunching factor of 0.27 and a form factor of 1.7. The sizes of the magnets are quite reasonable by this choice. One serious problem is that this injection emittance is based upon the following assumption. The painting emittance at the 400-MeV injection to the RCS is 144 π mm mrad, which grows by a factor of 1.5, being adiabatically damped to 54 π mm mrad. Since the RCS collimator acceptance is 324 π mm mrad, the extracted beams from the RCS can extend beyond this value of emittance. The beams located between 54 π mm mrad and 324 π mm mrad will be lost at the collimator located at the beam transport from the RCS to the MR. If the emittance growth is more than estimated, the beam loss at the collimator will limit the beam current. The emittances related to this matter are listed in Table. 1.5.

Table 1.4. Main parameters of the 50 GeV synchrotron.

Energy	50 GeV
Beam Intensity	3.3 x 10^{14} ppp
Repetition	0.3 Hz
Average Beam Current	15 μA
Beam Power	0.75 MW
Circumference	1567.5 m
Magnetic Rigidity	12.8 ~ 170 Tm
Lattice Cell Structure	Arc(3-Cell DOFO x 8 module) + Insertion(2-matching cell + 3-Straight Cell + 2-matching cell)
Typical Horizontal Tune	22.3
Typical Vertical Tune	17.3-22.3
Momentum Compaction Factor	-0.001 (imaginary γ_T)
Number of Bending Magnets	96 (5.85 m)
Magnetic Field	0.143 ~ 1.9 T
Total Number of Quadrupoles	216 (0.86,1.26, 1.46, 1.56, 1.66, 1.76, 1.86 m)
Number of Quadrupole Family	11
Maximum Field Gradient	18 T/m
Harmonic Number	9
RF Frequency	1.67 ~ 1.72 MHz
Beam Current (fundamental)	19 ~ 25 A
RF Voltage	280 kV
RF Voltage per Cavity	47 kV (16 kV/gap)
Number of RF Cavities	6
Beam Emittance at Injection	54 π mm mrad
Beam Emittance at Extractin (30 GeV)	10 π mm mrad
Beam Emittance at Extractin (50 GeV)	6.1 π mm mrad

Table 1.5. Emittance and acceptance (π mm mrad) in the MR cycle.

	Unnormalized Emittance	Normalized Emittance	Collimator Aperture	Physical Aperture
RCS				
Injection	144	146	324	486
Extraction	54	220		
BT from RCS to MR				
	54	220	54	120
MR				
injection	54	220	54~81	81
extraction (30 GeV)	10	330		81
extraction (50GeV)	6.1	330		81

It is also noted that the painting emittance for the MR injection cycle is by a factor of 1.5 less than that for the neutron production cycle. In other words, we have to change the painting emittance depending upon different cycles. The Laslett tune shift for the MR injection cycle is larger (- 0.22) than that for the neutron production cycle (- 0.16).

The slow extraction scheme is most difficult issue to solve for this kind of high-intensity, high-energy proton synchrotron. Only the one percent beam loss is allowed during the slow extraction process. An electrostatic septum (80 μmϕ tungsten wires with rhenium) is being developed for this purpose. The voltage of 230 kV, which is higher than the necessary value of 170 kV, has been already supplied to the electrodes. Although the beam simulation results satisfy the above requirement, the further improvement in the beam loss simulation will be necessary for increasing the margin, which is needed for this kind of the beam loss/radioactivity elimination.

The RF system of the MR will also use cavities loaded with the same MA as that of the 3-GeV ring. However, the Q value will be optimised for the MR. The adjustability of the Q value by cutting the MA core, which is also developed for this project, is another important advantage of the MA-loaded cavity.

1.6 Summary

The accelerator scheme for the high-intensity proton accelerator facility project in Japan is unique as follows. First of all, the RCS scheme is chosen for the MW proton machine producing the pulsed spallation neutrons. Second, the MR is attempting to realize the MW proton machine also for the several-GeV region. If successful, not only for the scientific and engineering output, but this accelerator complex will also open up the new era for the field of the accelerator technology. Together with the success of the SNS and/or ESS projects, this project will contribute a lot to the future several or ten MW accelerators, which are really required for the 21st century science and technology, including the biology, the particle physics, the energy development, the environmental science/technology and so forth.

For this purpose, there is no other way than challenging. On the other hand, we have to be careful and conservative, where we can. In this chapter we have briefly summarized how we are challenging and where we are conservative. In the following chapters, we will detail our design much more quantitatively.

References

[1] Y. Yamazaki, Proc. 1996 Linac Conf., 592 (1996).
[2] "The Joint Project for High-Intensity Proton Accelerators", KEK Report 99-4, JHF-99-3 and JAERI-Tech 99-056 (1999).
[3] Y. Yamazaki et al., "Accelerator Complex for the Joint Project of KEK/JHF and JAERI/NSP", Proc. 1999 Part. Accele. Conf., THDL1 (1999).
[4] Y. Yamazaki et al., "High Intensity Proton Accelerators for the JAERI/KEK Joint Project", Proc. 2000 European Accele. Conf., THOAF201(2000).
[5] T. Kato, KEK Report 96-17 (1997).
[6] Y. Yamazaki and T. Kato, Proc. 1998 Linac Conf., TU4011 (1998).
[7] Y. Yamazaki et al., "The Construction of the Low-Energy Front 60-MeV Linac for the JAERI/KEK Joint Project", Proc. 2000 Linac Conf., TUD07 (2000).
[8] T. Kageyama, Y. Yamazaki and K. Yoshino, Part. Accel. 32, 33(1990). T. Kageyama et al., Proc. 1994 Linear Accel. Conf. 248 (1994).
[9] K. Saito et al., KEK Report 89-21 (1990).
[10] N. Ouchi et al., Proc. 2000 Linac Conf., WE205 (2000).
[11] C. Ohmori et al., “High Field Gradient Cavity for JAERI-KEK Joint Project,” Proc. 8th European Part. Accel. Conf., 257(2002).